Enhanced mesenchymal stem cell differentiation on load-bearing trabecular nitinol scaffolds by medium perfusion

Th. Böse[1]*, R.E. Unger[1], H. Götz[2], I. Gotman[3], E.Y. Gutmanas[3], R. Tsaryk[4], and C.J. Kirkpatrick[1]

[1] REPAIRLab, Institute of Pathology, University Medical Center Mainz, Mainz, 55131 Germany
[2] ASMA Institute of Applied Structure- and Microsanalysis, Mainz, 55101 Germany
[3] Department of Materials Science and Engineering, Technion – Israel Institute of Technology, Technion City, Haifa, 3200003 Israel
[4] Max Planck Institute for Molecular Biomedicine, Münster, 48149 Germany

Trabecular nitinol (tNiTi) is a promising candidate material for bone tissue engineering applications mostly on account of its open-cell porous structure and elasticity, resembling natural bone. Generally, human mesenchymal stem cells (hMSC) can be seeded, cultivated and differentiated into cells of the osteogenic lineage on these scaffolds under static conditions. To determine if more biologically relevant scenarios influence hMSC we investigated the effect of medium perfusion on the osteogenic differentiation of hMSC grown on the tNiTi scaffolds. The scaffolds were seeded and cultivated in a commercial perfusion bioreactor system for four weeks. Following the cultivation and differentiation phase the cells were analyzed for the activity of alkaline phosphatase (ALP) and matrix mineralization. Medium perfusion enhanced osteogenesis in hMSC as well as the distribution of cells and extracellular matrix throughout the entire scaffold. Scanning electron microscopy analysis showed a co-localization of calcium and phosphate in the mineralized matrix. Furthermore, hMSC on perfused tNiTi scaffolds did not differentiate in the absence of dexamethasone (Dex), and osteogenesis in differentiating cells was not influenced by nickel ions released from the tNiTi scaffolds. Our data indicate that medium perfusion successfully supports the osteogenic differentiation of hMSC on porous tNiTi scaffolds.

Keywords: nitinol scaffolds, perfusion bioreactor, mesenchymal stem cells, osteogenic differentiation

1. Introduction

The osteogenic differentiation capability of human mesenchymal stem cells (hMSC) is an important feature of these cells that is being used in bone tissue engineering applications to develop strategies for the replacement of damaged or excised hard tissue. Furthermore, hMSC can be easily isolated from a patient and reimplanted as an autologous cell fraction, which makes them an attractive cell type for patient-specific tissue engineering approaches. One major focus in the development of such strategies is the application of MSC to a porous scaffold for bone tissue regeneration. During the last years many studies have demonstrated that the osteogenic differentiation of MSC was possible with different biomaterials, including hydrogels (i.e. collagen type 1 gels) [1, 2] metals (i.e. titanium) [3, 4] and ceramics (i.e. hydroxyapatite or tri-calcium phosphate) [5, 6]. Most studies focus on the use of biomaterials with properties mimicking natural bone, and it has been shown that the osteogenic differentiation of MSC is affected by the stiffness of such biomaterials [7–9]. In addition, a recently published study indicates that MSC possess a mechanical memory directly influencing the osteogenic differentiation through specific cell signaling [10].

Nitinol is a promising candidate biomaterial that exhibits a number of attractive properties, such as shape memory/superelasticity, high strength and good biocompatibility [11, 12]. Among the various metals and alloys that are used as implant materials in e.g. orthopaedics Nitinol offers the lowest modulus of elasticity, thus resulting in a low stress-shielding effect and therefore a reduced risk of implant loosening [13, 14]. Several investigations, including our previous study [15], have shown that hMSC differentiate into the osteogenic lineage when seeded on porous Nitinol scaffolds *in vitro* [15, 16]. However, these studies were performed under static cell culture conditions. It is known that static cultivation involves limitations in nutrient supply,

* *Corresponding author*
Thomas Böse, e-mail: boese@uni-mainz.de

as well as a reduced gas exchange on the scaffold, since the transport of substrates and waste products associated with cellular metabolism is limited by diffusion [17]. Furthermore, it has been shown that cell-seeded and *in vitro* cultivated 3D scaffolds are "encapsulated" by forming cell-matrix layers on the surface, mainly as a result of cell adherence to the scaffold periphery [18, 19]. This leads to dramatically reduced cell migration and penetration into the scaffolds and increased cell death in the central regions of the scaffold [20, 21]. To circumvent such an outcome perfusion bioreactors have been utilized in the last years, thus enabling an active and controllable medium transport, as well as an enhanced gas supply of perfused tissue constructs [17]. Moreover, it has been shown that hMSC respond to mechanical stimuli such as fluid flow and shear stress, resulting in increased proliferation and matrix production by cells [22, 23]. The combination of osteogenic differentiation medium, perfusion in 2D, as well as through 3D scaffolds stimulates an enhancement of osteogenesis at both the gene regulation and protein expression levels [24, 25]. Finally, dynamic cultivation combined with dynamic seeding strategies give enhanced cell distribution and uniformity of cell growth throughout the complete scaffold [26, 27].

The aim of the present study was to investigate the influence of medium perfusion on the osteogenic differentiation of hMSC seeded on trabecular nitinol scaffolds (tNiTi). This recently developed porous nitinol material possesses a unique open-cell structure, high strength and low stiffness, which make it an attractive scaffold for bone tissue regeneration in load-bearing locations [28]. Medium perfusion was applied in long-term cultivation of hMSC on tNiTi scaffolds and the deposition and distribution of matrix, as well as its calcification examined.

2. Materials and methods

2.1. Isolation and expansion of primary human mesenchymal stem cells

The isolation of primary human mesenchymal stem cells from 6 individual donors was performed as previously published [29]. Bone cells were processed strictly anonymously in accordance with local ethical regulations without recording patient-related data. The repeated washing of bone fragments with PBS (D8537, Gibco, Life Technologies, Darmstadt, Germany) resulted in a suspension containing loosely associated cell fractions and matrix. After filtration of the suspension through a 70 μm cell strainer (352350, BD Falcon, Heidelberg, Germany) cells were seeded at a density of 2×10^6 cells/cm^2 as passage 0 (P0) on uncoated T75 flasks (658175, Greiner Bio-One, Frickenhausen, Germany). The cultivation of P0 cells was carried out in DMEM/F-12 GlutaMax® (31331-028, Gibco, LifeTechnologies) containing 20% FBS (F7524, Sigma-Aldrich), 1% PenStrep (15140-122, Gibco, Life Technologies) and 5 ng/ml bFGF (F0291, Sigma-Aldrich). Medium was exchanged every day during the first week after isolation. After reaching approximately 80% confluence the cells were trypsinized (trypsin + 0.25% EDTA, 25200-056, Gibco, Life Technologies), washed with PBS and expanded at an initial cell seeding density of 5000 cells/cm^2. Cells in passages >0 were cultivated in DMEM/F-12 GlutaMax® containing 10% FCS, 1% PenStrep and 5 ng/ml bFGF (expansion medium). For all experiments cells were used in passages three to five.

2.2. Characterization of primary hMSC

The expanded cells were characterized for the expression of cell surface markers according to the guideline of the ISCT [30]. To perform this, cells were trypsinized, stained in an unfixed state according to the manufacturer's protocol for CD11b-FITC (11-0118-42, eBioscience), IgG1-FITC (11-4714, eBioscience), HLA-DR-APC (130-095-297), CD19-APC (130-091-248), CD34-FITC (130-081-001), CD45-FITC (130-080-202), CD73-APC (130-095-183), CD90-FITC (130-095-403), CD105-APC (130-094-926), CD44-FITC (130-095-195), CD29-APC (130-101-280), CD31-APC (130-092-652), IgG1-FITC (130-092-213), IgG2a-FITC (130-091-837), IgG1-APC (130-092-214), IgG2a-APC (130-091-836) (all from Miltenyi Biotec, Bergisch-Gladbach, Germany), and analyzed using a FACSCalibur flow cytometer (BD Bioscience) combined with CellQuestPro Software (BD Bioscience). Additionally, the cells were analyzed for their ability to differentiate into adipocytes, chondrocytes and osteoblasts. To achieve this, cells of each donor were seeded at a density of 2×10^4 cells/cm^2 in 24-well cell culture plates and cultivated in adipogenic (A10070-01, StemPro, Gibco, Life Technologies) or osteogenic differentiation medium (A10072-01, StemPro, Gibco, Life Technologies) for four weeks. Chondrogenic differentiation was studied in pellet cultures of 0.5×10^6 cells/pellet centrifuged at 400 g for 5 min and subsequently cultivated in chondrogenic differentiation medium (A10071-01, StemPro, Gibco, Life Technologies) for four weeks. Subsequently, cells were fixed with 3.7% paraformaldehyde (104005, Merck Millipore, Darmstadt, Germany) and stained with Oil-Red O (O9755, Sigma-Aldrich) for adipogenic differentiation and Alizarin-Red-S and Von Kossa's method (silver nitrate, 1015100050, Merck Millipore) for osteogenic differentiation, as published elsewhere [31].

2.3. Scaffold preparation

9 mm diameter discs were cut from 1.5 mm thick INCOFOAM® nickel foam sheet (1450 g/m^2 density, 590 μm cell size) and converted into tNiTi by PIRAC titanization at 900°C, 6 h. The detailed description of PIRAC titanization procedure can be found elsewhere [15, 28]. The scaffolds were sterilized at 2 bar and 121°C in an autoclave.

2.4. Dynamic cell seeding and cultivation

Perfusion-based cultivation of hMSC on tNiTi scaffolds was performed in a commercially available U-CUP-perfusion bioreactor (CellecBiotek AG, Basel, Swizerland). Each scaffold was seeded dynamically with 0.4672×10^6 hMSC ($= 2 \times 10^4$ MSC/cm^2) using a flow velocity of 1000 μm/s for 24 h as described previously [32]. Based on the given value of 0.013 cm^2/g for the specific surface of tNiTi scaffolds [28] a mean specific surface of 23.36 cm^2 (±0.798 cm^2) per scaffold was calculated from 5 scaffolds previously weighed to determine the total number of MSC to be seeded. The seeding procedure was conducted in expansion medium without the addition of bFGF. Cells of each biological replicate were seeded and cultivated separately. After the seeding process tNiTi scaffolds were transferred into fresh U-CUPs for dynamic cultivation or into upright T25 flasks for static cultivation. For the dynamic cultivation the flow velocity was reduced to 100 μm/s. The total working volume was kept constant for all conditions using a total volume of 7 ml. Medium exchange was performed once a week.

2.5. Induction of osteogenic differentiation

Osteogenic differentiation on tNiTi scaffolds was induced by adding 100 nM dexamethasone (D1756, Sigma-Aldrich), 10 mM β-glycerol phosphate (G9422, Sigma-Aldrich) and 50 μM ascorbic acid-2-phosphate (A8960, Sigma-Aldrich) to αMEM-GlutaMax® (32571-028, Gibco, Life Technologies) medium, supplemented with 10% FBS and 1% PenStrep, termed osteogenic differentiation medium (ODM) in this study. As control cultures cell-seeded tNiTi scaffolds were cultivated statically or dynamically in αMEM-GlutaMax® basal medium containing 10% FCS and 1% PenStrep (basal medium).

2.6. Alkaline phosphatase activity assay

The alkaline phosphatase (ALP) activity was assessed via quantification of the conversion of p-nitrophenyl phosphate (p-NPP) into p-nitrophenol (p-NP) by ALP. First, the cells were lysed in RIPA buffer as previously described [33]. The lysis was performed for 10 min on ice. The lysates were subsequently centrifuged at 14,000 rpm for 5 min. The protein concentrations were measured using the BCA Protein Assay kit (23225, Pierce, Thermo Scientific) according to the manufacturer's protocol. For the determination of ALP activity 20 μL of protein lysate were incubated with 60 μL of substrate solution (0.2% p-NPP (N4645, Sigma-Aldrich) dissolved in 1 M diethanolamine HCl (D8885, Sigma-Aldrich) pH 9.8) for 45 min at 37°C in a 96-multiwell plate (655101, Greiner Bio-One). The hydrolysis reaction was terminated by adding 80 μL of stop solution (0.2 mM EDTA (E5134, Sigma-Aldrich) in 2 M NaOH (106482, Merck Millipore) pH 8.0) to each well. The absorbance of each sample was measured in triplicate at a wavelength of 405 nm using a multiplate reader (GENios plus, TECAN). The activity of ALP was normalized to the protein concentration in each sample and defined as mmol p-NP/mg protein.

2.7. Quantification of total intracellular collagen content (TIC)

The TIC was quantified using the Sircol Collagen Assay (biocolor life science assays, Biolcolor Ltd., Carrickfergus, Northern Ireland, UK) according to the manufacturer protocol. The TIC was measured from protein lysates as prepared in the previous section (2.6. Alkaline phosphatase activity assay). Briefly, 100 μL of protein lysate were mixed with 1 ml of Sircol Dye Reagent supplied with the kit and incubated for 30 min at room temperature on a mechanical shaker. Subsequently, the samples were centrifuged at 12,000 rpm for 10 min. The resulting supernatant was discarded and the formed pallet was carefully coverd with 750 μL of ice-cold Acid-Salt Wash Reagent supplied with the kit. After another washing step (12,000 rpm, 10 min) 250 μL of Alkali Reagent (supplied with the kit) were added leading to the release of the bound dye. Following this, the absorbance at a wavelength of 550 nm was measured using a multiplate reader.

2.8. Quantification of matrix mineralization

The mineralization of matrix on tNiTi scaffolds was determined by quantification of calcium deposition using Calcium OCP Fluid 1+1-kit (Axiom Diagnostic, Worms, Germany) according to the manufacturer's protocol. Scaffold fragments were incubated in 1M HCl (X942.1, Karl Roth GmbH, Karlsruhe, Germany) for 15 min. After addition of the reagent mixture (R1 + R2 1/1) the absorption was measured at a wavelength of 560 nm (GENios plus, TECAN) in triplicate. The resulting calcium concentrations were normalized as total calcium amount per area of the related scaffold fragments. The total area was calculated based on the weight of the corresponding decellularized and heat-dried scaffold fragment compared to the total surface values for tNiTi scaffolds determined previously [15]. Additionally, matrix mineralization was quantified in 2D experiments with alizarin red using the Osteogenesis Quantification Kit (ECM815, Merck- Milipore). In brief, each well of a 24-well cell culture plate was fixed with 3.7% PFA for 10 min, washed twice with distilled water and subsequently covered with 500 μL alizarin red staining solution and incubated for 20 min. Afterwards, the staining solution was discarded and the wells were washed 3X with distilled water for 5 min each with gentle shaking. Following this the stain was extracted with 10% acetic acid for 20 min at room temperature. The alizarin red concentrations were determined by absorbance measurements at 405 nm with a multiwell plate reader (GENios plus, TECAN) using

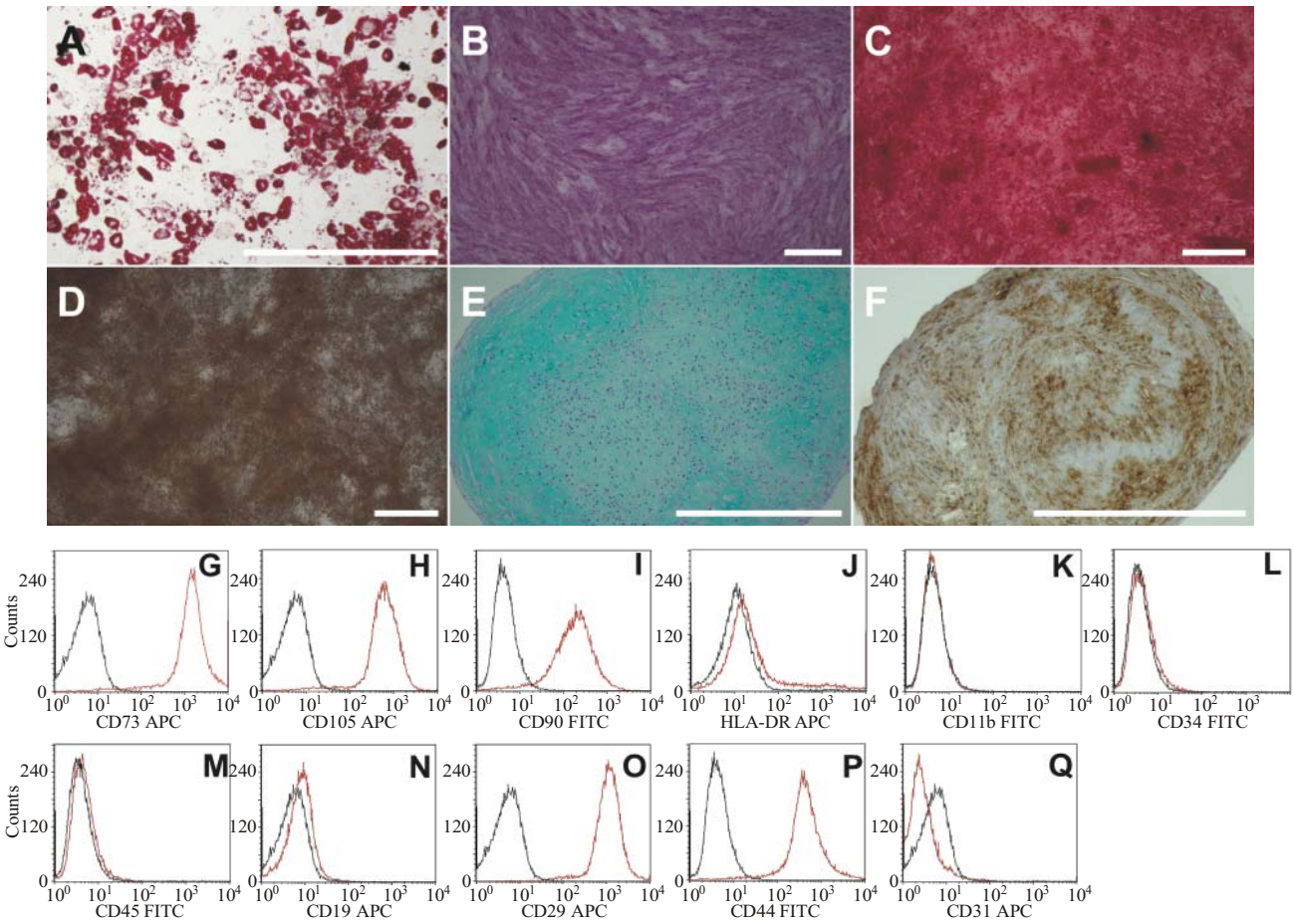

Fig. 1. Characterization of primary human mesenchymal stem cells isolated from trabecular bone: oil-red-O staining for oil droplet formation (A); fast-red-violet staining of ALP (B); alizarin red staining for calcium deposition (C); von Kossa staining for phosphate deposition (D); alcian blue staining of glycosaminoglycans (E); histochemical staining of aggrecan (F); scale bars 200 μm; G–R—analysis of surface marker profile by flow cytometry: CD73 (G), CD105 (H), CD90 (I), HLA-DR (J), CD11b (K), CD34 (L), CD45 (M), CD19 (N), CD29 (O), CD44 (P), CD31 (Q); red lines indicate cell populations with the corresponding marker expression; black lines indicate isotype controls.

a standard curve of alizarin red staining solution prepared in a 10% acetic acid solution as well.

2.9. Immunofluorescence staining and stereomicroscopy

For immunofluorescence staining scaffolds were washed with PBS and fixed with 3.7% PFA for 10 min. The staining procedure was performed as previously described [34] using rabbit-anti-human collagen-1 as primary antibody (1 : 50, T40103R, Meridian Life Science, Memphis, TN, USA) and a donkey-anti-rabbit secondary antibody (1 : 200, A21206, Invitrogen, Life Technologies, Darmstadt, Germany). Fluorescence images were obtained using a Keyence BZ-9000 fluorescence microscope (Keyence Deutschland GmbH, Montabaur, Germany). Stereomicroscopy was performed using a MF205 FA stereomicroscope, (Leica Microsystems, Heidelberg, Germany). In brief, samples to be analyzed were washed 3X with distilled water and subsequently air-dried for 30 min at 37°C in a steaming cabinet.

2.10. Scanning electron microscopy (SEM) and energy-dispersive X-ray analyses (EDX)

Samples were prepared as for stereomicroscopy. SEM and EDX were performed using a QUANTA 200 FEG field emission electron microscope (FEI, Hillsboro, OR, USA) coupled with an INCA Energy 350 energy-dispersive X-ray analysis system (Oxford Instruments Analytical GmbH, Uedem, Germany), containing an INCA X-Sight Si(Li) Platinum detector. SEM was performed at ultra-high vacuum mode using a voltage of 20 kV.

2.11. Statistical analysis

All experiments were repeated with 3 biological replicates including 2 scaffolds per group. The results are presented as means ± standard error (SEM). For quantitative measurements (protein concentration, ALP activity, calcium concentrations) 3 technical replicates were performed. The analysis of matrix mineralization using SEM and EDX was

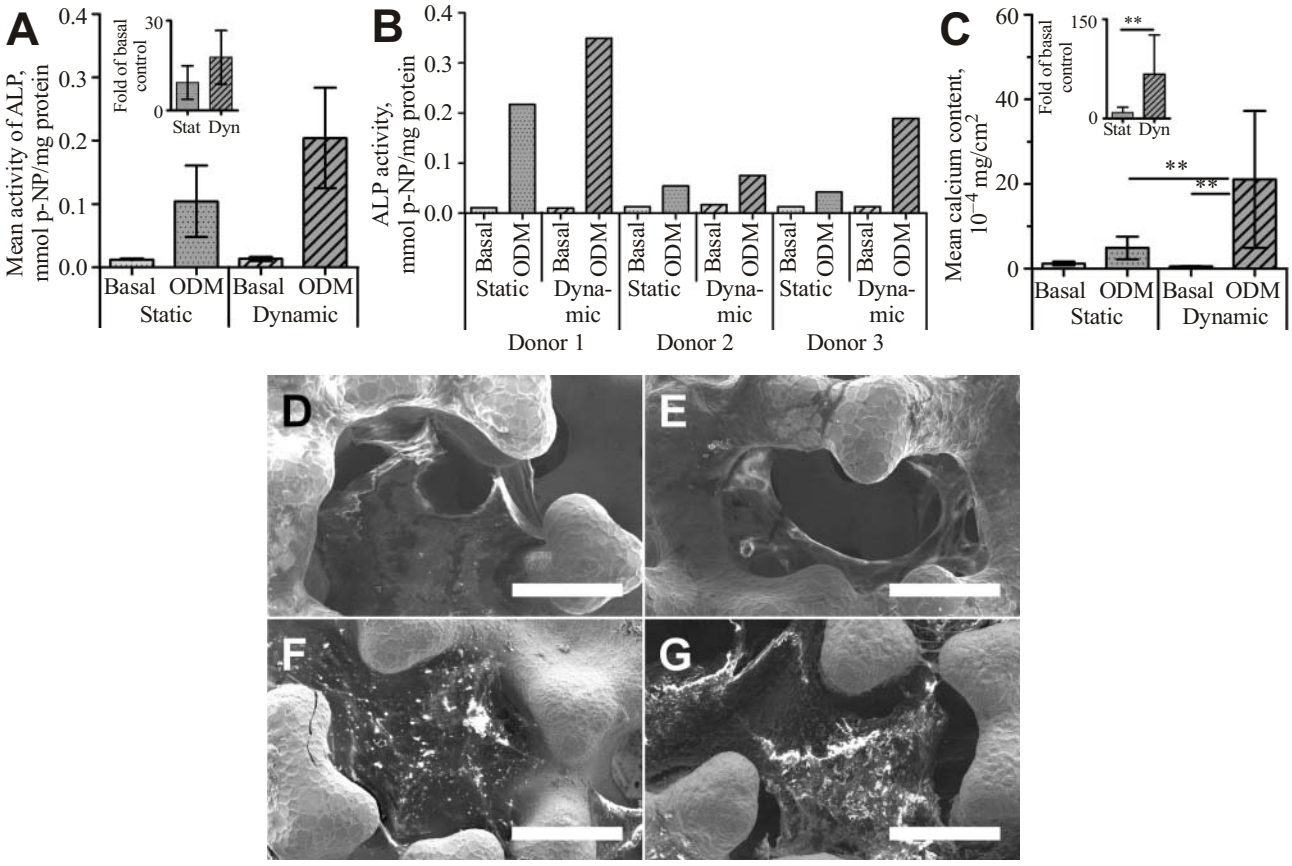

Fig. 2. Determination of ALP activity and calcium deposition in static and perfused cultures and their corresponding basal controls: A—ALP activity shown as mean values of three different donors, the small insert graph compares ALP activity of static and dynamic cultures normalized to the respective basal controls: B—although statistical significance could not be demonstrated, a common trend towards enhanced ALP activity due to flow is indicated at the single donor level; C—determination of the calcium content in the secreted matrix as mean values from three donors ($n = 3$), the small insert graph compares the calcium deposition in static and dynamic differentiation samples normalized to the respective basal controls. Asterisks indicate statistically significant changes (** = $p < 0.01$); D—SEM on static basal sample; E—SEM on dynamic basal sample; F—SEM on static ODM sample; G—SEM on dynamic ODM sample; scale bars 200 μm.

performed exemplarily on 1 donor. Statistical analysis was performed in Microsoft Excel using the paired student's t-test for the comparison of couples of experimental groups. No global statistical analysis was performed. The normal distribution of the data was investigated using the Analyse-it® tool for Microsoft Excel. No statistical evaluation was performed on data shown on the single donor level or on data obtained by EDX.

3. Results

3.1. Characterization of mesenchymal stem cells

To characterize the cells used in this study the guidelines of the International Society for Cell Therapy (ISCT) for characterization of MSC were followed [30]. The cells isolated by the protocol as described in the method section exhibited multilineage differentiation potential as well as a profile of surface markers as recommended by the guideline paper. Thus, following the inductive cultivation in adipogenic, osteogenic and chondrogenic medium the cells showed clear evidence of adipogenic, osteogenic and chondrogenic differentiation (Fig. 1—exemplarily shown for one donor—this donor further corresponds to "Donor 1" in Fig. 2). The formation of oily droplets was shown by positive oil-red-O staining (Fig. 1A). The fast-red-violet stain, the alizarin-red stain and the von Kossa stain demonstrated the increased expression of alkaline phosphatase as well as the deposition of calcium and phosphate in the osteogenic differentiation samples (Figs. 1B–1D). Chondrogenic differentiation in pellet cultures was shown by a strong alcian blue staining reaction as well as by a positive localization of aggrecan (Figs. 1E and 1F). Additional FACS analyses revealed that the cells were highly positive for the expression of CD73, CD90, CD105, CD29 and CD44 (Figs. 1G, 1H, 1I, 1O, and 1P). In contrast, the same cells were found to be negative for the expression of the cell surface mark-

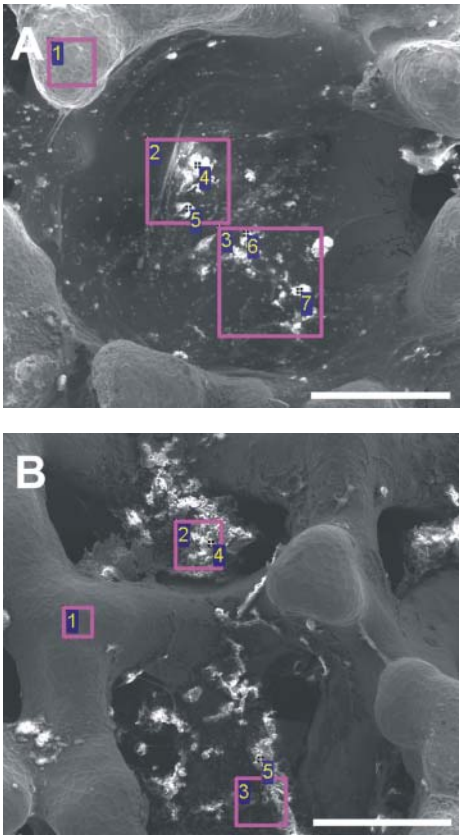

Suppl. Fig. 1. Differential formation of calcium phosphate minerals in the calcified matrix of static and dynamic culture samples: A—static osteogenic differentiation; B—dynamic osteogenic differentiation; numbers indicate region of interest (ROI) analyzed by EDX–magenta rectangles indicate area-based EDX analyses. ROI 4-7 in A and 4 and 5 in B represent single point EDX analyses for the co-localization of calcium and phosphorus. Scale bars 200 μm.

ers HLA-DR, CD11b, CD34, CD45, CD19 and CD31 (Figs. 1J–1N and 1Q, respectively). Our findings are in accordance with the suggested minimal criteria for the characterization of mesenchymal stem cells as defined in the ISCT guidelines. Therefore, the cells isolated by our protocol were considered to be human mesenchymal stem cells (hMSC).

3.2. Static versus dynamic differentiation

hMSC were cultivated under comparative static and dynamic conditions in either basal medium or osteogenic differentiation medium (ODM) for four weeks and subsequently analyzed for the expression of the osteogenic proteins alkaline phosphatase, collagen type 1 and for mineralization of the secreted matrix. Cultivation of hMSC in ODM medium led to a 3- to 20-fold increase in ALP activity compared to the basal controls. A further 1.3- to 4-fold enhancement under dynamic differentiation conditions compared to static differentiation conditions was observed, whereas no change was detectable between static or dynamic basal controls (Fig. 2A). The effect was not statistically significant but was observed for all investigated donors (Fig. 2B). The same trend was found when determining the amount of calcium deposition in the newly formed and mineralized matrix. Under static differentiation conditions calcium levels were only slightly increased (e.g. donor 2: 1.93×10^{-4} mg/cm^2 (basal control) compared to 2.05×10^{-4} mg/cm^2 (static ODM)). In contrast, a statistically significant 2- to 5-fold increase in calcium deposition was observed in dynamic differentiation samples compared to the static ones (Fig. 2C). Furthermore, the formation of minerals in the extracellular matrix could be visualized by scanning electron microscopy and appeared to be more abundant under dynamic differentiation conditions (SEM, Figs. 2D and 2E). No formation of minerals in the extracellular matrix of static and dynamic basal cultures was detected (SEM, Figs. 2F and 2G).

3.3. Analysis of matrix mineralization

To confirm matrix mineralization, energy-dispersive X-ray analysis (EDX) was used to obtain a qualitative evaluation of minerals formed [35]. Overview images obtained by SEM clearly indicated the existence of minerals in the extracellular matrix (Figs. 2D and 2E). Exemplary EDX analyses ($n = 1$) on rectangular and single-point regions of interest (ROI) detected a co-localization of calcium and phosphorus in all samples cultivated in ODM (Supplemen-

Suppl. Table 1. Exemplary determination of the atomic content of calcium and phosphorus in areas and at single points represented in Suppl. Fig. 1. The obtained data correspond to Donor 4 shown in Fig. 5

Differentiation condition	Region of interest	Calcium, at %	Phosphorus, at %
Static basal control	Not shown	0.00	0.00
Dynamic basal control	Not shown	0.00	0.00
Static ODM	1 (area, material)	0.00	0.00
	2 (area)	1.17	1.01
	3 (area)	1.83	1.36
	4 (single point)	1.74	1.54
	5 (single point)	1.42	0.94
	6 (single point)	0.53	0.58
	7 (single point)	1.37	0.99
Dynamic ODM	1 (area, material)	0.00	0.00
	2 (area)	2.96	2.63
	3 (area)	2.66	2.53
	4 (single point)	2.50	2.27
	5 (single point)	4.53	4.20

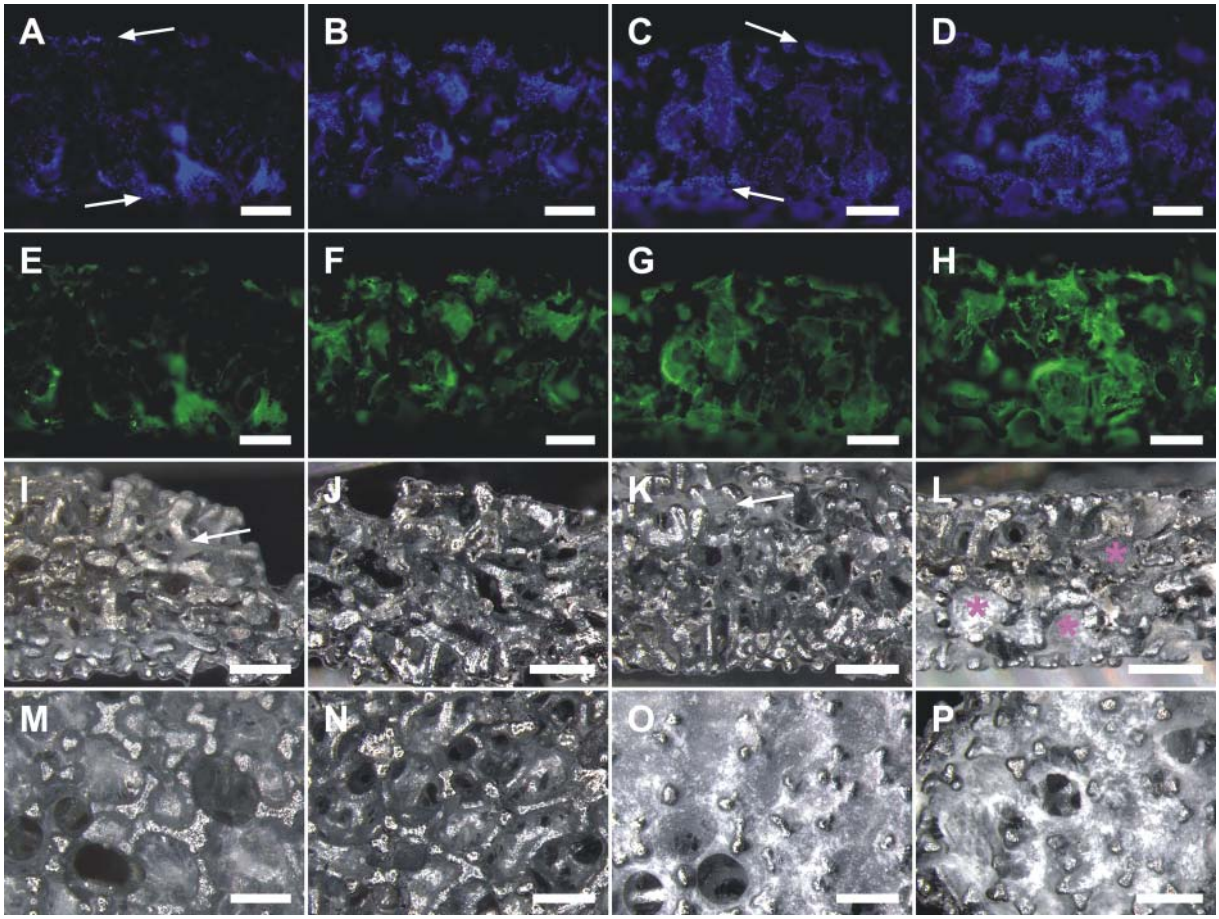

Fig. 3. Analysis of mesenchymal stem cell growth and distribution of osteogenic matrix on trabecular NiTiNOL scaffolds cultivated under comparative static and dynamic culture conditions for four weeks. Image data correspond to Donor 1 shown in Fig. 2B: A, E, I, M—static basal control; B, F, J, N—dynamic basal control; C, G, K, O—static differentiation; D, H, L, P—dynamic differentiation. Analysis of cell distribution using DAPI cell nuclei stain (A–D); distribution of collagen type 1 (E–E); stereomicroscopic evaluation of distribution of calcified matrix (I–L); stereomicroscopic overview of the scaffold surface (M–P). Arrows indicate predominant growth areas in static samples (A, C, I, K). Asterisks indicate highly calcified areas in the scaffold center (L). Scale bars 500 μm.

tary Fig. 1) whereas no calcium phosphate deposits were detectable in the static or dynamic basal controls (Supplementary Table 1).

3.4. Analysis of cell and matrix distribution

Following the quantitative and qualitative analysis of matrix mineralization a study of the distribution and composition of matrix formed by hMSC throughout the tNiTi scaffold body in response to medium perfusion was performed. It is known that perfusion cultivation results in an enhanced distribution and uniformity of cellular matrix on three dimensional scaffolds [36]. The distribution of cells visualized by a DAPI cell nuclear stain is shown in Figs. 3A–3D. In scaffolds cultivated under dynamic conditions an improved distribution of cells was found (Figs. 3B and 3D), with high numbers of cells observed in the inner portions of the scaffold, whereas cell growth was predominantly limited to the surface regions in statically cultivated scaffolds (Figs. 3A and 3C). Immunofluorescent staining for collagen type 1, one of the principal proteins in natural bone, showed a similar distribution. Figures 3E–3H demonstrate that osteogenic differentiation resulted in an increased fluorescence signal for collagen type 1 compared to the basal controls. It is important to note that this collagenous matrix was mostly found on the scaffold surface in the static samples (Figs. 3E and 3G), whereas the perfused samples showed an increased fluorescence signal in the scaffold center (Figs. 3F and 3H). A similar behavior was detected in all individual donors (Fig. 3 corresponds to Donor 1; for Donor 2 and 3 see Supplementary Figs. 2 and 3, respectively). For the microscopic evaluation of the matrix calcification an ODM- and perfusion-dependent tendency was observed. Calcified matrix was found to be distributed over the total scaffold depth under dynamic differentiation conditions, as detected by stereomicroscopic analyses of scaffold cross sections (Figs. 3I–3L). Strongly calcified matrix was found in the

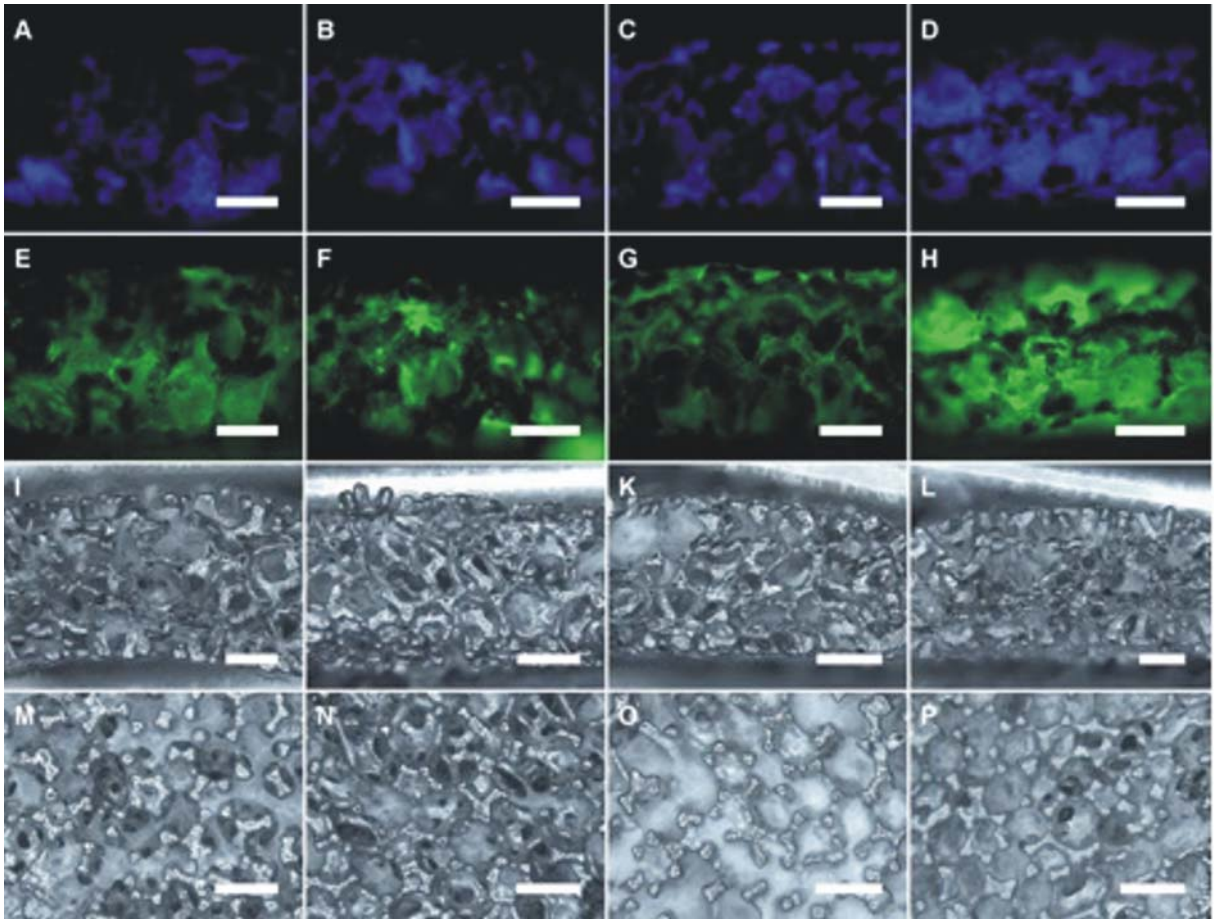

Suppl. Fig. 2. Analysis of mesenchymal stem cell growth and distribution of osteogenic matrix on trabecular NiTiNOL scaffolds cultivated under comparative static and dynamic culture conditions for four weeks. Data correspond to Donor 2 shown in Fig. 2B. A, E, I, M—static basal control; B, F, J, N—dynamic basal control; C, G, K, O—static differentiation; D, H, L, P—dynamic differentiation. Analysis of cell distribution using DAPI cell nuclei stain (A–D); distribution of collagen type 1 (E–H); stereomicroscopic evaluation of distribution of calcified matrix (I–L); stereomicroscopic overview of the scaffold surface (M–P). Arrows indicate predominant growth areas in static samples (A, C, I, K), asterisks indicate highly calcified areas in the scaffold center (L). Scale bars 500 μm.

scaffold center, as well as on the surface of tNiTi scaffolds cultivated under dynamic differentiation conditions (Figs. 3L and 3P). On the other hand, calcified matrix was found to be limited to the scaffold surface of statically differentiated samples (Figs. 3K and 3O). The same surface-limited matrix deposition was found on tNiTi scaffolds of the corresponding basal controls (Figs. 3I and 3M). In the dynamically cultivated basal controls the deposition of matrix occurred in a close range along the trabeculae of the tNiTi scaffolds and was therefore hardly visible on stereomicroscopy (Figs. 3J and 3N).

3.5. Osteogenic differentiation in hMSC in the absence of Dex

Having shown stronger differentiation potential of hMSC under dynamic conditions, we investigated whether medium perfusion through tNiTi scaffolds could serve as a mechanical inducer of osteogenesis in our MSC cultures. For this, the above described perfusion experiments were repeated, but omitting dexamethasone (ODM-Dex) from the ODM, a synthetic glucocorticoid able to induce osteogenic differentiation in MSC cultures [37]. After 4 weeks of cultivation the activity of ALP as well as the deposition of calcium was found to be clearly decreased in ODM-Dex cultures compared to the standard differentiation samples (Figs. 4A, 4B and 4C, 4D). The levels for ALP activity and calcium in ODM-Dex cultures were comparable to the corresponding basal controls of each donor (Figs. 4A and 4B). Furthermore, SEM analyses of the extracellular matrix showed an absence of the formation of minerals in the static ODM-Dex cultures as well as in the dynamic ODM-Dex cultures (Figs. 5C and 5D, respectively). Therefore, medium perfusion on its own through tNiTi scaffolds did not induce mineralization of extracellular matrix produced by hMSC. In contrast, the evaluation of matrix deposition represented by collagen type 1 staining revealed an increased

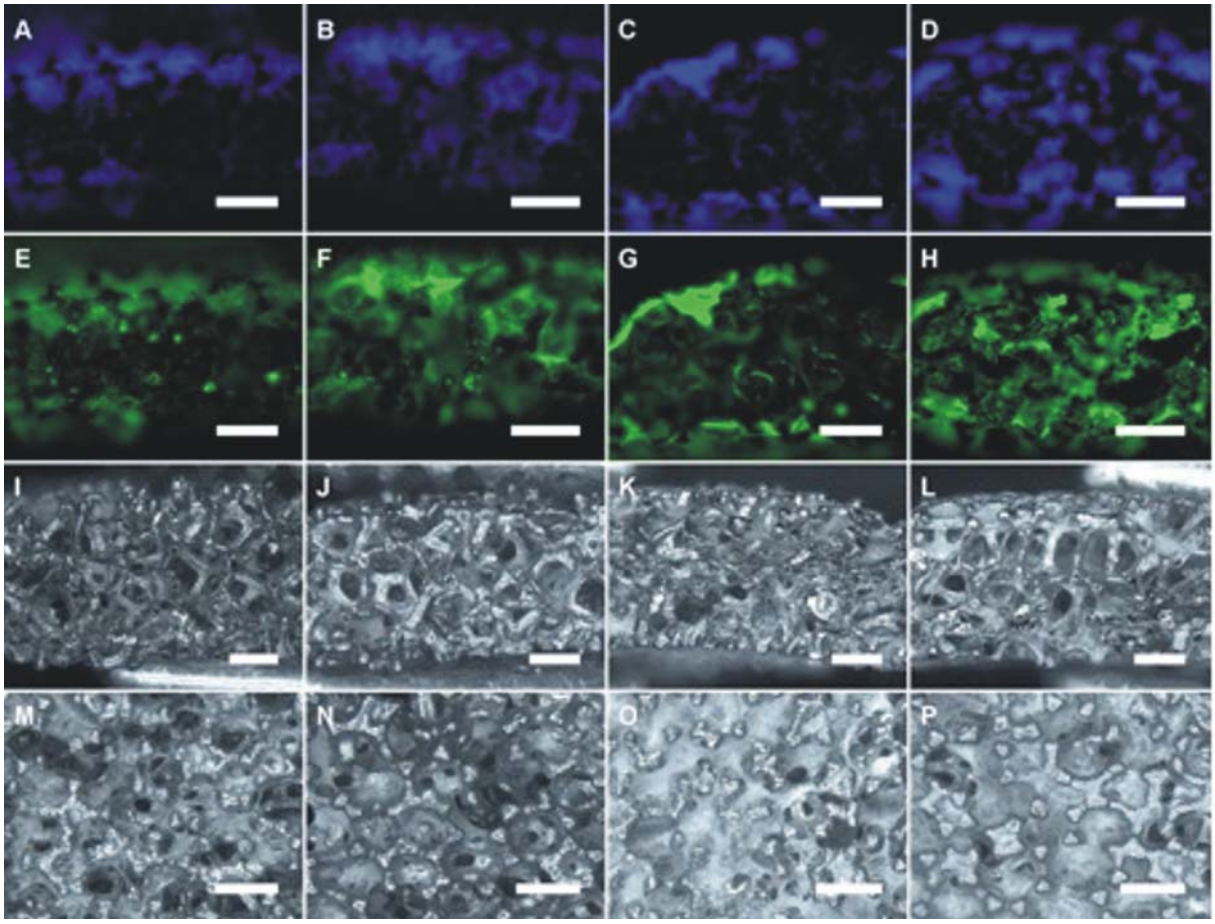

Suppl. Fig. 3. Analysis of mesenchymal stem cell growth and distribution of osteogenic matrix on trabecular NiTiNOL scaffolds cultivated under comparative static and dynamic culture conditions for four weeks. Data correspond to Donor 3 shown in Fig. 2B. A, E, I, M—static basal control; B, F, J, N—dynamic basal control; C, G, K, O—static differentiation; D, H, L, P—dynamic differentiation. Analysis of cell distribution using DAPI cell nuclei stain (A–D); distribution of collagen type 1 (E–H); stereomicroscopic evaluation of distribution of calcified matrix (I–L); stereomicroscopic overview of the scaffold surface(M–P). Arrows indicate predominant growth areas in static samples (A, C, I, K), asterisks indicate highly calcified areas in the scaffold center (L). Scale bars 500 μm.

deposition in ODM-Dex cultures compared to scaffolds cultivated in basal medium (Fig. 5E versus 5G, Fig. 5H versus 5J). This increase in ODM-Dex was observed under both static and dynamic differentiation conditions. However, the deposition of collagen type 1 in ODM-Dex samples was slightly enhanced when scaffolds were perfused (Fig. 5G versus 5J), which indicated a possible effect of medium perfusion on the expression of collagen type 1 in hMSC on tNiTi. This trend was common among all investigated donors (Supplementary Fig. 4, Supplementary Fig. 5) and was underlined by the quantification of the TIC in static Basal, ODM and ODM-Dex cultures (Fig. 5A). Comparable to the increase of the immunofluorescence signal for collagen type 1 an increased TIC was detected in dynamic ODM-Dex cultures compared to the corresponding dynamic basal controls or the static ODM-Dex cultures (Fig. 5A). These results are consistent at the single donor level (Fig. 5B) indicating that medium, perfusion affects the expression of collagens. Furthermore, the quantification of the TIC shows a general trend towards the expression of enhanced TIC levels when MSC-seeded tNiTi scaffolds were cultivated in ODM in which medium perfusion led to an additional increase of the TIC (Fig. 5A). Although no statistical significance was detectable this effect was found to be consistent in all investigated donors (Fig. 5B).

4. Discussion

In the present study using a commercial perfusion bioreactor system we investigated the influence of medium perfusion through trabecular Nitinol scaffolds on the osteogenic differentiation of primary hMSC. In a previous study we demonstrated that hMSC differentiate into cells of the osteogenic lineage on tNiTi, as shown by enhanced ALP activity and calcium deposition on the scaffolds compared to plastic controls [15]. However, since the experiments in the previous study were performed under static conditions

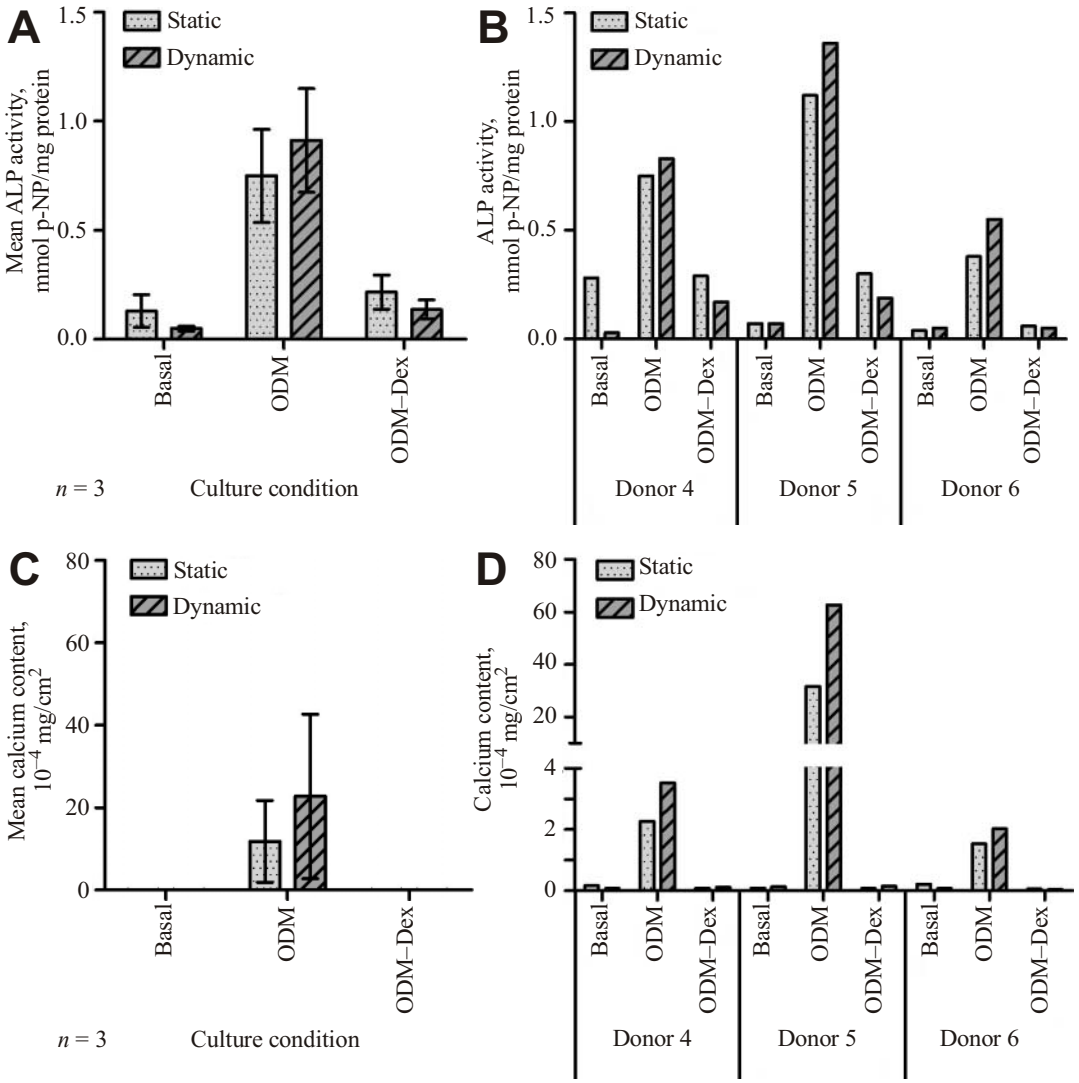

Fig. 4. Evaluation of the osteogenic inductivity of medium perfusion in the absence of dexamethasone: A—determination of the mean ALP activity from 3 biological replicates (±SEM), the small insert graph compares ALP activity in static and dynamic ODM and ODM-Dex cultures normalized to the respective basal controls; B—ALP activity shown at single donor level; C—determination of the mean calcium content in the extracellular matrix from 3 biological replicates (±SEM), the small insert graph compares the mean calcium content in static and dynamic ODM and ODM-Dex cultures normalized to the respective basal controls; D—calcium content shown at single donor level.

we were interested in determining if medium perfusion through these scaffolds could enhance the osteogenic differentiation process. The hMSC that were used for the flow-based investigations showed an expression pattern of surface markers, as well as the trilineage differentiation potential as recommended by the ISCT guideline [30]. In addition, based on the marker constellation subpopulations of hematopoietic stem or progenitor cells, adult hematopoietic cells and endothelial cells could be excluded.

To study the support of tNiTi scaffolds for the osteogenic differentiation of hMSC in response to medium perfusion cell-seeded scaffolds were cultivated under comparative static and dynamic conditions in a perfusion bioreactor. Since it is known that medium perfusion through three-dimensional scaffolds may increase the distribution and uniformity of the growing and differentiating cells, as well as of the formed matrix [36, 38]. Our results support these findings by showing increased ALP activities, mineralization of deposited collagen matrix and the distribution thereof on tNiTi scaffolds when medium perfusion is applied. In the static samples cell growth as well as matrix deposition were predominantly limited to the scaffold surface and peripheral region. A similar outcome was shown by other groups for statically cultivated and differentiated 3D scaffolds [18]. It is important to note that all scaffolds used in the present study were dynamically seeded to give cell-loaded scaf-

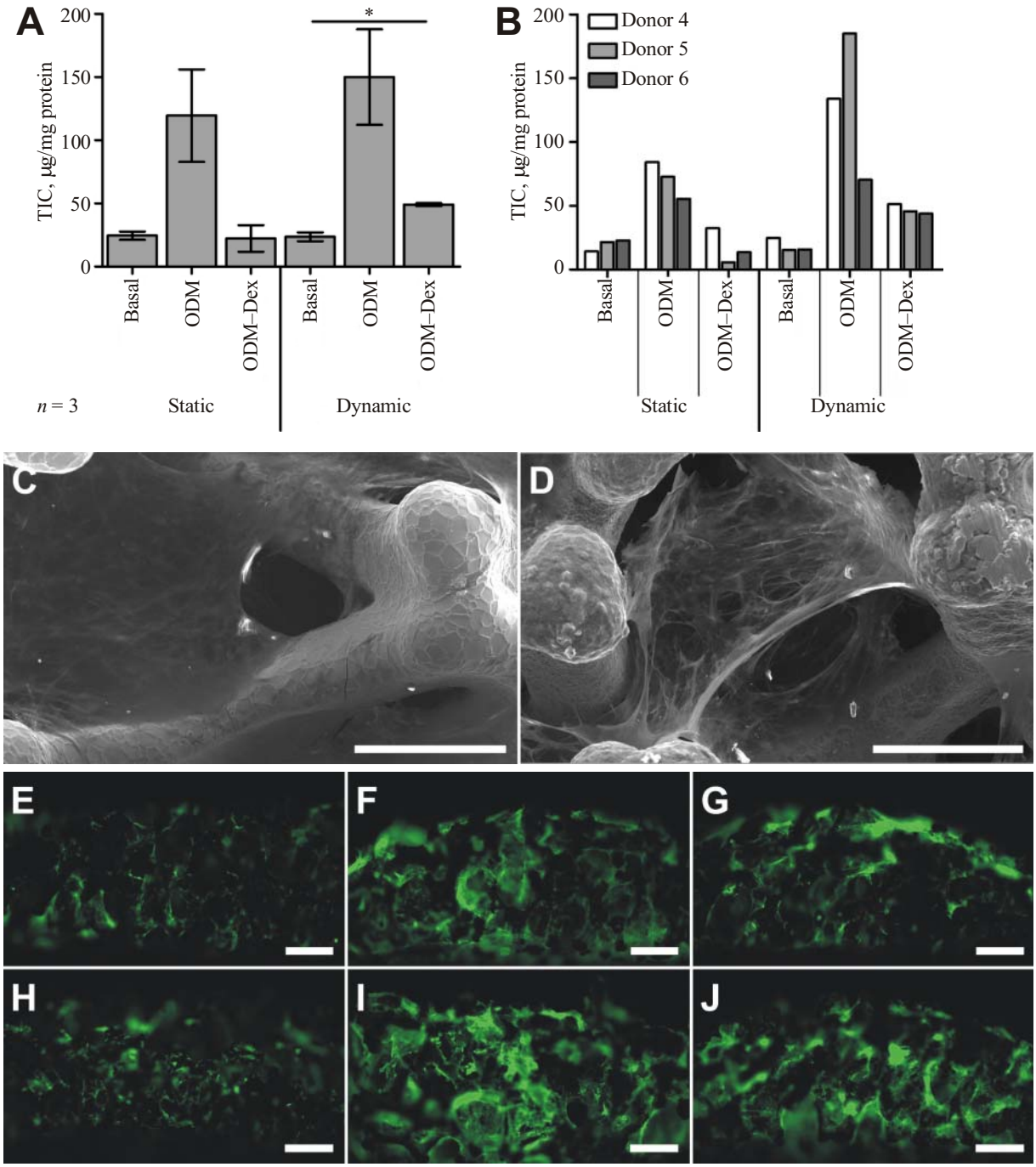

Fig. 5. Evaluation of the osteogenic inductivity of medium perfusion in the absence of dexamethasone: A—determination of total intracellular collagen content (TIC) from 3 biological replicates; B—determination of TIC at single donor level; statistically significant differences are indicate by asterisks "*": $p < 0.05$. No evidence of mineral formation on the extracellular matrix of static (C) and dynamic (D) differentiation samples cultivated in the absence of dexamethasone, scale bars = 200 µm; E–G—determination of collagen type 1 deposition on tNiTi scaffolds under static conditions: static basal (E), static ODM (F), static ODM–dexamethasone (G), scale bars 500 µm; H–J—collagen type 1 deposition on tNiTi scaffolds under dynamic conditions: dynamic basal (H), dynamic ODM (I), dynamic ODM–dexamethasone (J); E–J correspond to Donor 4 shown in Fig. 5B, 5D and Fig. 6B; scale bars 500 µm.

folds with a comparable cell distribution pattern at the baseline level. Therefore, it is likely that cell death in the central areas of the scaffolds and migration to the scaffold periphery occur in all static samples as previously described [19]. In contrast, enhanced cell growth, intracellular collagen expression, matrix deposition and calcification as well

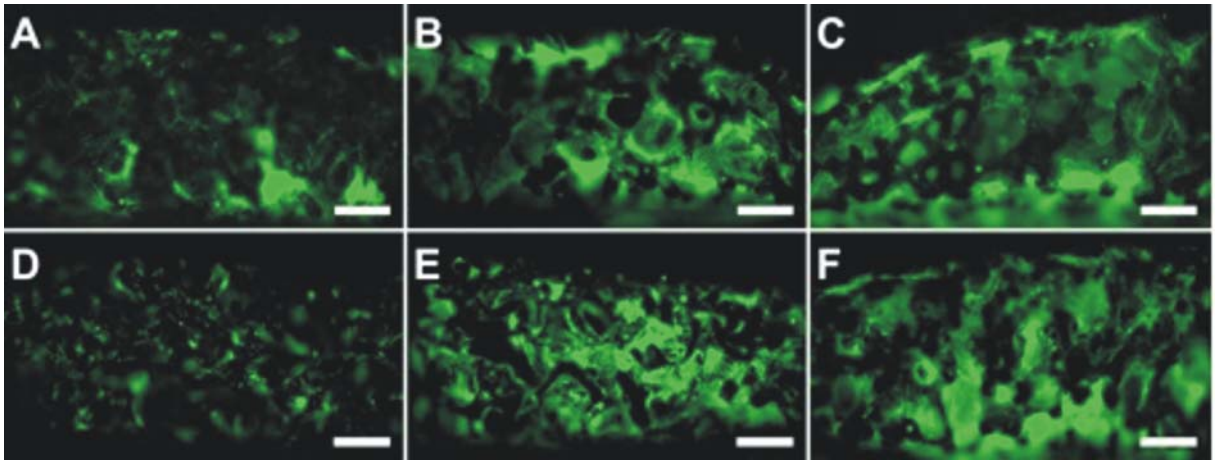

Suppl. Fig. 4. Evaluation of the osteogenic inductivity of medium perfusion in the absence of dexamethasone. Data correspond to Donor 5 shown in Figs. 5B, 5D and Fig. 6B. A–C—determination of collagen type 1 deposition on tNiTi scaffolds under static conditions: static basal (A), static ODM (B), static ODM–dexamethasone (C). Scale bars = 500 μm. D–F—collagen type 1 deposition on tNiTi scaffolds under dynamic conditions: dynamic basal (D), dynamic ODM (E), dynamic ODM–dexamethasone (F). Scale bars 500 μm.

as the more homogeneous distribution of cells in dynamic cultures showed that medium perfusion clearly had a beneficial effect on the osteogenic differentiation of hMSC on tNiTi scaffolds. However, the question remained concerning whether this effect of medium perfusion was a result of better cell distribution or whether medium flow could serve as a mechanical stimulus to induce osteogenesis in hMSC. The latter has been shown to occur with rat MSC [39]. Holtorf et al. investigated the osteogenic differentiation of rat MSC in the absence of dexamethasone (Dex) while adding ascorbic acid (AA) and â-glycerol phosphate (β-GP) to the cell culture medium [39]. Matrix calcification, as well as enhanced ALP activity was found in the absence of Dex when medium perfusion was applied. In contrast, in the present studies human MSC did not show enhanced ALP activities or calcification when cultivated in the absence of Dex (ODM-Dex cultures) on tNiTi scaffolds, although similar concentrations of AA and β-GP were used as in the rat MSC study. Furthermore, these parameters were not influenced by the application of medium perfusion in our experiments.

Another study on the effects of perfusion on MSC showed enhanced mRNA levels of bone sialoprotein (BSP), bone morphogenic protein-2 (BMP-2) and osteopontin (OP) in response to medium flow [40]. The response to medium flow was observed even in basal medium without the addition of AA or β-GP [40]. However, the authors did not show a similar result at the protein level. Thus, it is not clear if these enhanced levels were of biological relevance to the

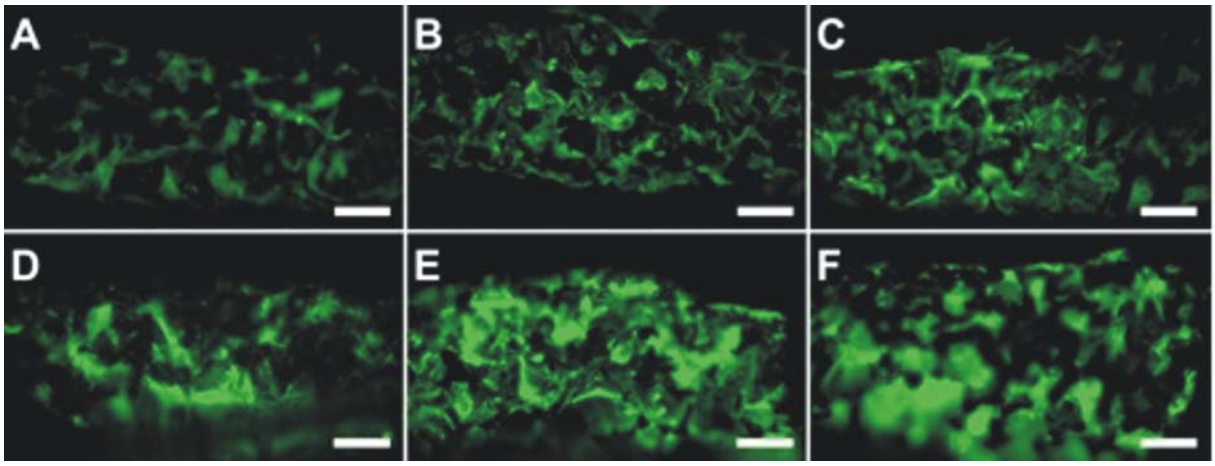

Suppl. Fig. 5. Evaluation of the osteogenic inductivity of medium perfusion in the absence of dexamethasone. Data correspond to Donor 6 shown in Figs. 5B, 4D and Fig. 6B. A–C—determination of collagen type 1 deposition on tNiTi scaffolds under static conditions: static basal (A), static ODM (B), static ODM–dexamethasone (C), scale bars 500 μm; D–F—collagen type 1 deposition on tNiTi scaffolds under dynamic conditions: dynamic basal (D), dynamic ODM (E), dynamic ODM–dexamethasone (D). Scale bars 500 μm.

osteogenic differentiation of hMSC. In the present study medium perfusion in the absence of Dex led to the increase of the TIC as well as the collagen type 1 deposition by hMSC on tNiTi. Therefore, mechanical stimuli provided by the medium perfusion could also contribute to osteogenic differentiation of hMSC while supporting the expression and secretion of collagen to the extracellular matrix. However, it did not lead to full differentiation of hMSC, since matrix calcification was not observed on tNiTi scaffolds cultivated dynamically in the absence of Dex. A possible explanation is that in the present system medium perfusion acted as a co-stimulus to Dex, where both the effects of medium flow on the distribution of cells and nutrients and the mechanical effect on the osteogenic differentiation would be of importance. This mechanical effect could be concluded from the SEM analysis and stereomicroscopic observations of statically and dynamically differentiated hMSC on tNiTi scaffolds, which showed a morphologically differential, more evenly distributed and increased mineralization on the surface, as well as in the center of dynamically differentiated tNiTi scaffolds. Additionally, the atomic levels of calcium and phosphorus as detected by EDX were enhanced in dynamic cultures compared to the static situation. Although a detailed atomic analysis of the mineralization by EDX was performed primarily on one donor the general trend from the EDX quantification is in accordance with the trend found for the quantification of calcium and TIC. Moreover, ALP activity was found to be increased in all dynamic differentiation samples compared to the static ones. Although further studies were not carried out on possible mechanisms or other ranges of flow velocities it appears that medium perfusion acted synergistically with the inductive effect of Dex in our system. The flow velocity used in the present study was lower (100 μm/s in 8 mm perfused diameter resulting in a theoretical flow rate of 0.3 ml/min) than the value used by Holtdorf and colleagues (1 ml/min) [39]. Hence, the comparability of the conclusion reached in our study with the conclusion obtained by Holtdorf et al. is difficult. Accordingly, it is not clear whether medium perfusion through tNiTi scaffolds could enhance the osteogenic differentiation of hMSC even in the absence of Dex to ODM when a flow rate of 1 ml/min was used. Additional studies are needed to investigate this issue. In this study medium perfusion had a positive effect on the osteogenic differentiation of hMSC and mineralization on tNiTi. The outcome of our previous study [15] proving tNiTi to be a suitable candidate as a biomaterial in bone tissue engineering is further highlighted by the behavior of tNiTi under dynamic conditions as described in the present study. Such pre-cultivation of cell-seeded tNiTi scaffolds in a perfusion bioreactor could be envisaged as a promising strategy in the application of tNiTi as a bone substitute material. Similar observations were made for scaffolds manufactured from other materials like hydroxyapatite [41] or poly(L-lactic acid) [42]. Nevertheless, enhanced mineralization on tNiTi obtained by cultivation of hMSC under perfusion is an important step forward towards the application of this material in bone tissue engineering.

5. Conclusion

The present study investigated the osteogenic differentiation of hMSC on tNiTi scaffolds under medium perfusion. The results demonstrate that osteogenic differentiation of hMSC takes place on tNiTi scaffolds, thus providing a possibility to generate cell-loaded tNiTi constructs for bone tissue engineering applications. Furthermore, the use of medium perfusion represents a powerful tool to optimize the cellular environment of the hMSC needed for an adequate osteogenic differentiation process, as medium perfusion through tNiTi scaffolds enhanced the distribution of extracellular matrix and differentiating cells and also increased the degree of mineralization. In addition, it appears that medium perfusion could act as a mechanical stimulus in a synergistic manner with biological inducers of osteogenesis, such as dexamethasone. *Summa summarum*, the cultivation of cell-loaded tNiTi scaffolds in a perfusion bioreactor positively influenced the differentiation of hMSC and therefore favors tNiTi as a promising biomaterial for bone tissue engineering applications.

Competing interests

The authors declare no personal or financial conflict of interests.

Author's contributions

TB designed the study, performed experimental lab work, data analyses and wrote the manuscript. REU supervised study design, coordinated the study and participated in drafting the manuscript. HG participated in data aquisition using SEM and EDX and interpretation of data. IG and EYG produced the scaffolds and participated in drafting the manuscript. RT participated in study design and interpretation of data and participated in drafting the manuscript. CJK participated in coordination of the study, the interpretation of data and participated in drafting the manuscript. All authors gave final approval for publication.

Acknowledgements

The authors thank the core facility "Microscopy" at the Institute for Molecular Biology IMB, Mainz, Germany, for the professional support in the acquisition of stereomicroscopic images.

Funding

This research was supported by the German-Israeli Foundation for Scientific Research and Development (G.I.F), Grant No. 1092-28.2/2010.

References

1. Schneider RK, Puellen A, Kramann R, Raupach K, Bornemann J, Knuechel R, et al. The osteogenic differentiation of adult bone marrow and perinatal umbilical mesenchymal stem cells and matrix remodelling in three-dimensional collagen scaffolds. Biomaterials. 2010; 31: 467–480.
2. Yu HS, Won JE, Jin GZ, Kim HW. Construction of mesenchymal stem cell-containing collagen gel with a macrochanneled polycaprolactone scaffold and the flow perfusion culturing for bone tissue engineering. Biores Open Access. 2012; 1: 124–136.
3. Zhao L, Liu L, Wu Z, Zhang Y, Chu PK. Effects of micropitted/nanotubular titania topographies on bone mesenchymal stem cell osteogenic differentiation. Biomaterials. 2012; 33: 2629–2641.
4. Stiehler M, Lind M, Mygind T, Baatrup A, Dolatshahi-Pirouz A, Li H, et al. Morphology, proliferation, and osteogenic differentiation of mesenchymal stem cells cultured on titanium, tantalum, and chromium surfaces. J Biomed Mater Res A. 2008; 86: 448–458.
5. Lin L, Chow KL, Leng Y. Study of hydroxyapatite osteoinductivity with an osteogenic differentiation of mesenchymal stem cells. J Biomed Mater Res A. 2009; 89: 326–335.
6. Wang C, Duan Y, Markovic B, Barbara J, Howlett CR, Zhang X, et al. Phenotypic expression of bone-related genes in osteoblasts grown on calcium phosphate ceramics with different phase compositions. Biomaterials. 2004; 25: 2507–2514.
7. Gobaa S, Hoehnel S, Roccio M, Negro A, Kobel S, Lutolf MP. Artificial niche microarrays for probing single stem cell fate in high throughput. Nat Methods. 2011; 8: 949–955.
8. Shih YR, Tseng KF, Lai HY, Lin CH, Lee OK. Matrix stiffness regulation of integrin-mediated mechanotransduction during osteogenic differentiation of human mesenchymal stem cells. J Bone Miner Res. 2011; 26: 730–738.
9. Emaus N. Serum level of under-carboxylated osteocalcin and bone mineral density in early menopausal women. Osteoporosis Int. 2010; 21: S703.
10. Yang C, Tibbitt MW, Basta L, Anseth KS. Mechanical memory and dosing influence stem cell fate. Nat Mater. 2014; 13: 645–652.
11. Castleman LS, Motzkin SM, Alicandri FP, Bonawit VL. Biocompatibility of nitinol alloy as an implant material. J Biomed Mater Res. 1976; 10: 695–731.
12. Kapanen A, Ryhanen J, Danilov A, Tuukkanen J. Effect of nickel-titanium shape memory metal alloy on bone formation. Biomaterials. 2001; 22: 2475–2480.
13. Greiner C, Oppenheimer SM, Dunand DC. High strength, low stiffness, porous NiTi with superelastic properties. Acta Biomater. 2005; 1: 705–716.
14. Geetha M, Singh AK, Asokamani R, Gogia AK. Ti based biomaterials, the ultimate choice for orthopaedic implants—A review. Prog Mater Sci. 2009; 54: 397–425.
15. Gotman I, Ben-David D, Unger RE, Bose T, Gutmanas EY, Kirkpatrick CJ. Mesenchymal stem cell proliferation and differentiation on load-bearing trabecular Nitinol scaffolds. Acta Biomater. 2013; 9: 8440–8448.
16. Strauss S, Dudziak S, Hagemann R, Barcikowski S, Fliess M, Israelowitz M, et al. Induction of osteogenic differentiation of adipose derived stem cells by microstructured nitinol actuator-mediated mechanical stress. PLoS One. 2012; 7: e51264.
17. Plunkett N, O'Brien FJ. Bioreactors in tissue engineering. Technol Health Care. 2011; 19: 55–69.
18. Glowacki J, Mizuno S, Greenberger JS. Perfusion enhances functions of bone marrow stromal cells in three-dimensional culture. Cell Transplant. 1998; 7: 319–326.
19. Goldstein AS, Juarez TM, Helmke CD, Gustin MC, Mikos AG. Effect of convection on osteoblastic cell growth and function in biodegradable polymer foam scaffolds. Biomaterials. 2001; 22: 1279–1288.
20. Cartmell SH, Porter BD, Garcia AJ, Guldberg RE. Effects of medium perfusion rate on cell-seeded three-dimensional bone constructs in vitro. Tissue Eng. 2003; 9: 1197–1203.
21. Ishaug-Riley SL, Crane-Kruger GM, Yaszemski MJ, Mikos AG. Three-dimensional culture of rat calvarial osteoblasts in porous biodegradable polymers. Biomaterials. 1998; 19: 1405–1412.
22. Delaine-Smith RM, Reilly GC. Mesenchymal stem cell responses to mechanical stimuli. Muscles Ligaments Tendons J. 2012; 2: 169–180.
23. Riddle RC, Taylor AF, Genetos DC, Donahue HJ. MAP kinase and calcium signaling mediate fluid flow-induced human mesenchymal stem cell proliferation. Am J Physiol Cell Physiol. 2006; 290: C776–C784.
24. Kreke MR, Huckle WR, Goldstein AS. Fluid flow stimulates expression of osteopontin and bone sialoprotein by bone marrow stromal cells in a temporally dependent manner. Bone. 2005; 36: 1047–1055.
25. Kavlock KD, Goldstein AS. Effect of pulse frequency on the osteogenic differentiation of mesenchymal stem cells in a pulsatile perfusion bioreactor. J Biomech Eng. 2011; 133: 091005.
26. Wendt D, Marsano A, Jakob M, Heberer M, Martin I. Oscillating perfusion of cell suspensions through three-dimensional scaffolds enhances cell seeding efficiency and uniformity. Biotechnol Bioeng. 2003; 84: 205–214.
27. Koch MA, Vrij EJ, Engel E, Planell JA, Lacroix D. Perfusion cell seeding on large porous PLA/calcium phosphate composite scaffolds in a perfusion bioreactor system under varying perfusion parameters. J Biomed Mater Res A. 2010; 95: 1011–1018.
28. Gotman I. Fabrication of load-bearing NiTi scaffolds for bone ingrowth by Ni foam conversion. Adv Eng Mater. 2010; 12: B320–B325.
29. Kolbe M, Xiang Z, Dohle E, Tonak M, Kirkpatrick CJ, Fuchs S. Paracrine effects influenced by cell culture medium and consequences on microvessel-like structures in cocultures of mesenchymal stem cells and outgrowth endothelial cells. Tissue Eng Part A. 2011.
30. Dominici M, Le Blanc K, Mueller I, Slaper-Cortenbach I, Marini FC, Krause DS, et al. Minimal criteria for defining multipotent mesenchymal stromal cells. The International Society for Cellular Therapy position statement. Cytotherapy. 2006; 8: 315–317.
31. Pittenger MF, Mackay AM, Beck SC, Jaiswal RK, Douglas R, Mosca JD, et al. Multilineage potential of adult human mesenchymal stem cells. Science. 1999; 284: 143–147.
32. Sadr N, Pippenger BE, Scherberich A, Wendt D, Mantero S, Martin I, et al. Enhancing the biological performance of synthetic polymeric materials by decoration with engineered, de-

cellularized extracellular matrix. Biomaterials. 2012; 33: 5085–5093.
33. Tsaryk R, Peters K, Barth S, Unger RE, Scharnweber D, Kirkpatrick CJ. The role of oxidative stress in pro-inflammatory activation of human endothelial cells on Ti6Al4V alloy. Biomaterials. 2013; 34: 8075–8085.
34. Tsapikouni T, Garreta E, Melo E, Navajas D, Farre R. A bioreactor for subjecting cultured cells to fast-rate intermittent hypoxia. Respir Physiol Neurobiol. 2012; 182: 47–52.
35. Bonewald LF, Harris SE, Rosser J, Dallas MR, Dallas SL, Camacho NP, et al. von Kossa staining alone is not sufficient to confirm that mineralization in vitro represents bone formation. Calcif Tissue Int. 2003; 72: 537–547.
36. Wendt D, Marsano A, Jakob M, Heberer M, Martin I. Oscillating perfusion of cell suspensions through three-dimensional scaffolds enhances cell seeding efficiency and uniformity. Biotechnology and Bioengineering. 2003; 84: 205–214.
37. Grigoriadis AE, Heersche JN, Aubin JE. Differentiation of muscle, fat, cartilage, and bone from progenitor cells present in a bone-derived clonal cell population: effect of dexamethasone. J Cell Biol. 1988; 106: 2139–2151.
38. Liao JH, Guo XA, Nelson D, Kasper FK, Mikos AG. Modulation of osteogenic properties of biodegradable polymer/extracellular matrix scaffolds generated with a flow perfusion bioreactor. Acta Biomaterialia. 2010; 6: 2386–2393.
39. Holtorf HL, Jansen JA, Mikos AG. Flow perfusion culture induces the osteoblastic differentiation of marrow stromal cell-scaffold constructs in the absence of dexamethasone. J Biomed Mater Res A. 2005; 72: 326–334.
40. Yourek G, McCormick SM, Mao JJ, Reilly GC. Shear stress induces osteogenic differentiation of human mesenchymal stem cells. Regen Med. 2010; 5: 713–724.
41. Bjerre L, Bunger C, Baatrup A, Kassem M, Mygind T. Flow perfusion culture of human mesenchymal stem cells on coralline hydroxyapatite scaffolds with various pore sizes. J Biomed Mater Res A. 2011; 97: 251–263.
42. Alvarez-Barreto JF, Landy B, VanGordon S, Place L, DeAngelis PL, Sikavitsas VI. Enhanced osteoblastic differentiation of mesenchymal stem cells seeded in RGD-functionalized PLLA scaffolds and cultured in a flow perfusion bioreactor. J Tissue Eng Regen Med. 2011; 5: 464–475.